A Novel Adaptive Control Approach for Maximum Power-Point Tracking in Photovoltaic Systems

energies

MDPI

Article

A Novel Adaptive Control Approach for Maximum Power-Point Tracking in Photovoltaic Systems

Muhammad Ahmed Qureshi [1], Francesco Torelli [2], Salvatore Musumeci [1], Alberto Reatti [3], Andrea Mazza [1] and Gianfranco Chicco [1,*]

[1] Dipartimento Energia "Galileo Ferraris", Politecnico di Torino, 10129 Torino, Italy; muhammad.qureshi@polito.it (M.A.Q.); salvatore.musumeci@polito.it (S.M.); andrea.mazza@polito.it (A.M.)
[2] Dipartimento Ingegneria Elettrica e dell'Informazione, Politecnico di Bari, 70125 Bari, Italy; francesco.torelli@poliba.it
[3] Dipartimento Ingegneria dell'Informazione, University of Florence, 50139 Firenze, Italy; alberto.reatti@unifi.it
* Correspondence: gianfranco.chicco@polito.it

Abstract: Maximum power-point tracking (MPPT) is applied to enable effective operation of photovoltaic (PV) systems under different external conditions. MPPT is based on a control system that aims at maintaining the PV system operation in the most effective conditions of maximum power output. This paper demonstrates the effective application of a novel adaptive control approach developed to be used in the field of power electronics. The application to MPPT is developed by using a non-inverted Buck-Boost converter applied to the PV system. The novel control methodology is based on the application of the Lyapunov stability concepts. The strength of this novel control technique is confirmed by the accurate comparison among the results obtained by using the proposed solution and some controllers proposed in the literature.

Keywords: photovoltaic plant; maximum power-point tracker; Buck-Boost converter; Lyapunov theory; model reference adaptive control; Torelli control box

Citation: Qureshi, M.A.; Torelli, F.; Musumeci, S.; Reatti, A.; Mazza, A.; Chicco, G. A Novel Adaptive Control Approach for Maximum Power-Point Tracking in Photovoltaic Systems. *Energies* **2023**, *16*, 2782. https://doi.org/10.3390/en16062782

Academic Editors: Salvatore Lombardo and Santiago Silvestre

Received: 6 February 2023
Revised: 3 March 2023
Accepted: 14 March 2023
Published: 16 March 2023

1. Introduction

Nowadays, renewable energy is a crucial factor for sustainable technological development. Photovoltaic (PV) systems are currently among the most sustainable and continuously improving solutions to exploit renewable energy sources. PV systems are used in several applications for stand-alone and grid-connected electrical networks. It is implemented for residential, commercial, industrial, or rural supply applications [1–3]. Furthermore, the PV generation may be used in powered infrastructures for electrical vehicle (EV) charging stations [4,5]. Moreover, grid-connected PV plants with batteries as the energy storage elements are used to stabilize and back up energy in the modern electric network [6].

A general structure of a PV system, shown in Figure 1, consists of a PV array, a reference voltage generator, a DC–DC converter and a controller. In order to extract the maximum power from the PV array under the conditions of varying temperature and irradiance levels, the PV array needs to be operated at its maximum power-point (MPP). It is the job of the MPPT controller to ensure that the PV array is operated at the MPP by controlling the choppers' duty cycle. This tracking of MPP by the controller is aptly called Maximum Power-Point Tracking (MPPT) [7]. The MPPT for photovoltaic (PV) systems is a typical application of power electronics. The MPPT controller is an extremely important part of the PV system, since the efficiency of the controller determines the efficiency of the whole PV system under variable external conditions.

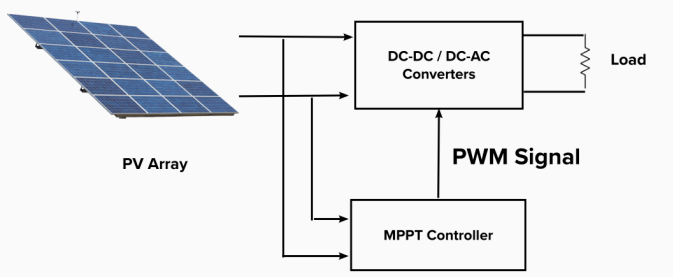

Figure 1. PV system with MPPT control.

In a PV system, the energy efficiency improvement depends on two different aspects:

- The technological structure of the PV cells and layout arrangement [8].
- The algorithm used to increase the energy extracted from the PV source by using MPPT [9].

Several MPPT techniques have been proposed and implemented in the literature. A comprehensive overview of the MPPT techniques used in the literature has been presented in the Refs. [10,11]. The commonly proposed techniques in the literature can be broadly categorized as follows:

- Hill-climbing techniques;
- Optimization based algorithms;
- Artificial intelligence-based techniques; and
- Linear and non-linear techniques.

Hill-climbing (HC) techniques such as Perturb and Observe (P&O) and Incremental Conductance (IC) have existed in the literature for decades. These HC techniques are popular because of their relatively accurate results, ease of implementation and low number of sensors needed.

In P&O, the input power of the converter is calculated, then the voltage level is perturbed by a small amount (ΔV) in one direction by varying the duty cycle. If the resulting change in power (ΔP) is positive, then the perturbation is continued in that direction, otherwise it is reversed. In this way, the MPP is eventually reached. There are two problems associated with P&O, which could make P&O inefficient. First of all, after every perturbation, the power cannot be measured until the transients have been completed, and this increases the overall rate of convergence. Secondly, although the rate of convergence can be increased by increasing the amplitude of the perturbation, with higher amplitudes of perturbation the amplitude of the oscillations around the MPP would also increase, which results in higher power losses. To overcome these issues, modified P&O strategies have been developed [12]. In these modified strategies, novel procedures have been adopted to modify the perturbation value so that the speed of convergences can be increased. To improve the P&O performance in partial shading conditions, the conventional P&O algorithm has been modified in different ways. For example, in the Ref. [13] a first tuning of the duty-cycle of the converter between the maximum and minimum feasible values was introduced, so that all the peaks can be identified, while in the Ref. [14] the entire exploration range was divided into rectangular areas and the rectangles were further divided into smaller rectangles, then the area with the highest possible chance of finding the GMPP was selected. In both cases, the overall time of convergence increased, and in the latter case there is still a chance that the GMPP is not reached if an inaccurate section is chosen. In other cases, the conventional P&O algorithm was combined with metaheuristic algorithms such as particle swarm optimization [15] and ant colony optimization [16], obtaining improved results and a marked decrease in power oscillations.

In IC, the aim is to make the sum of instantaneous conductance (I_{pv}/V_{pv}) and incremental conductance ($\Delta I_{pv}/\Delta V_{pv}$) equal zero [17]. The operating method is the same as for P&O, as the duty cycle is again varied to search for MPP. Under rapidly variable environmental conditions, IC provides more precise tracking and better adaptability to varying

environmental conditions than P&O. However, once again, it faces similar problems as P&O, namely a trade-off between the perturbation amplitude and the oscillations power loss. Furthermore, it has around the same efficiency as P&O but requires more complex control circuitry which leads to higher cost [10]. To improve the IC algorithm performance in partial shading conditions, the conventional algorithm was modified in the Ref. [18] to obtain a simple linear equation to track the GMPP. However, this algorithm requires the use of additional measurement circuits at the output of the converter, thus increasing the overall cost.

In the last years, the use of artificial intelligence (AI) to enhance both the MPPT algorithms and the production and management systems of the PV components has increased the PV plant efficiency [19]. Bio-inspired AI optimization-based techniques (or meta-heuristics) have become popular as alternatives to Hill-climbing algorithms [20,21]. An advantage of these algorithms is their possible superior performance under partial shading conditions [22]. When the entire PV array is under uniform irradiance, the power-voltage curve only shows a single peak that is then tracked by the MPPT controller. However, under partial shading conditions, that is, when a PV array is under non-uniform irradiance conditions (due to a shadow on part of a PV panel or cloudy weather), the power-voltage curve shows multiple peaks. Only one of these peaks has the highest value which is then the GMPP, while other peak points are called Local MPPs (LMPPs). In this case, the task of the controller becomes more challenging as it additionally needs to make sure that it converges to the GMPP instead of the LMPP peaks present. One major issue with hill climbing techniques is that since these techniques are designed to search for a peak without taking into account the global response, they tend to converge on the LMPP instead of the GMPP [20].

The structure of these meta-heuristics algorithms is quite similar. The first step is the random generation of unique *particles* or *individuals* in the solution space, to form a population of particles. The positions of each particle are evaluated against an objective function. These particles then interact with each other to produce new *offsprings*. If the position of the offspring is better than its parent, the position is updated. In this way, the cycle continues until the process converges to the desired point. These meta-heuristic algorithms offer better performance in rapidly varying the environmental conditions in terms of response time, overshoot and fluctuations, but most importantly, they are useful for trying to converge to the GMPP under partial shading conditions [21].

However, the advantages of meta-heuristic algorithms come at a cost. First of all, the performance of these algorithms is highly dependent on the initial conditions and selected parameters. For example, the selection of the size of the initial population is critical to having an accurate balance between exploration (ability to accurately search at a global level) and exploitation (accurate convergence on the local maxima). Higher population size increases exploration but decreases exploitation, and vice versa [23]. In fact, the ideal population size is a function of the peaks in the PV characteristic curves. This means that a certain population size that is ideal for a certain PV array system will not be suitable for another PV system.

Some techniques randomize or use non-linearly decreasing initial weight parameters of the *individuals* to initially enhance the exploration process before optimizing the exploitation process in steady-state conditions [24]. However, this step increases the computation burden of the operation and increases the overall cost. Selection of the parameters of the algorithm also plays an important part in the performance of these controllers.

Other AI-based techniques, such as fuzzy logic (FL) and neural networks (NN)-based controllers tend to handle system non-linearities better than conventional methods. These techniques do not require knowledge of the mathematical model of the system. A FL controller consists of three parts: (i) fuzzification, (ii) decision-making, and (iii) defuzzification. During the fuzzification part, a membership function is used to convert numerical input variables into linguistic variables. The input variables are typically the error (e) and the change in error (Δe). In the case of converters, the errors can be the

instantaneous values of power or voltage. The decision-making stage consists of a rule base as determined by the designer of the system. In the de-fuzzification stage, a membership function is again used to convert a linguistic variable to a numerical output. For a FL-based MPPT, the output is normally the duty cycle of the DC–DC converter. The main advantages of a FL-based MPPT are that it does not need an accurate model of the PV system, can handle system non-linearities, and can work with imprecise inputs [25]. However, their main disadvantages are the requirement of setting up the parameters of the fuzzy controller, and the complex computations during their implementation.

A NN-based controller, similarly to a FL-based controller, operates like a black box and does not require any information about the PV system. The input parameters, in the case of a NN-based MPPT algorithm, can be voltages and currents, or other environmental parameters. The output is usually the duty cycle. In order to accurately track the MPP, the NN needs to establish an accurate relationship between the input and output parameters. This relationship is established by training the system for an extended period of time and/or with an appropriate training data set [11]. Another important point to note is that since each PV array has a different characteristic, a NN will have to be trained separately for each PV array. Additionally, since the characteristics of a PV array get modified with time, the NN will have to be periodically trained to keep accurate tracking of the MPP. Although both FL-based and NN-based controllers have been successful in providing accurate and fast dynamic responses even in harsh environmental conditions, there remain the issues of computational cost, implementation complexity, and time-consuming processes for training the NN [26].

Because of the problems mentioned above, linear controllers have been proposed for MPPT. Linear techniques such as proportional-integral-derivative (PID) controllers are used to extract maximum power from PV systems by optimization of the control gains [27]. The main issue with linear controllers is that, as mentioned before, PV arrays and DC–DC converters are inherently non-linear systems and thus the use of linear controllers requires the construction of small-signal approximated models of the PV system, to linearize the system around the equilibrium point.

Non-linear controllers, on the other hand, guarantee the robustness and stability of systems for different operational conditions [28]. This is why non-linear controllers have been the focus of recent research for applications to PV systems. In recent years, various non-linear controllers have been implemented for tracking the MPP in PV systems, based on *back-stepping*, *sliding mode* control (SMC) and its derivative techniques [22,29–31]. Their control is easier to implement in digital form and techniques such as SMC in particular offer appropriate performance against sensitivity to system parameter variations or load voltage fluctuations.

However, even for these non-linear control techniques there are certain issues that need to be addressed. For example, there is a well-known issue of the "chattering" phenomenon which can lead to additional power losses in practical implementation of SMC for practical applications. For power converters, there is another challenge that needs to be addressed. For the ideal implementation of SMC, the switching frequency should be kept very high. However, for certain practical purposes, the frequency has to be maintained at a certain constant value and cannot be increased to high values due to additional component costs of components and filter design issues. This problem is solved by implementing the equivalent control of SMC using the PWM technique that keeps the operating frequency constant. However, then, operating at finite fixed frequency leads to greater steady-state errors. This issue was first tackled in the Ref. [32] through the introduction of an "integral of error" term as a control variable. This is called Integral Sliding Mode Control (ISMC) and this methodology reduces the steady-state errors. Since then, the sliding mode control with additional integral action has also been used for the regulation of Čuk and Quasi-Z-source converters [28,33].

The use of higher-order terms is not just reduced to sliding-mode only. The same methodology has been used in the Ref. [30] to reduce the steady-state error and improve

upon the results of a back-stepping controller implemented for MPPT by the Ref. [29]. However, the problem with the use of this methodology is that it not only increases the computational burden of the system, but also requires additional knowledge of the time derivatives of the variables.

Following the method used to implement efficient non-linear controllers, this paper proposes a novel "model-reference adaptive control" (MRAC) for MPP tracking in a PV system. The rationale of the choice is that the adaptive control technique can be quite useful for systems that have parameters that can undergo fluctuations. In the literature, adaptive control techniques have been applied to different engineering fields, such as robotics [34], flight control [35,36], power system control [37] and so forth. The control mechanism of the proposed approach is based on the Torelli Control Box (TCB) methodology, in which the convergence of the error vectors to the equilibrium point is ensured through the fulfilment of the Lyapunov stability criteria. The TCB methodology has been conceptualized to be used for different mathematical programming problems [38], and has been applied to various problems in the power systems area, to solve the power flow [39], the optimal power flow [40], and the formulation of differential algebraic equations in the analysis of distribution networks [41] or switched capacitor converters [42].

The novel application to the MPPT controller with the proposed TCB-based control approach has been developed for a non-inverted Buck-Boost converter-based system for interfacing a PV source with a DC system.

The next sections of this paper are organized as follows. Section 2 shows the mathematical formulation for the proposed MRAC approach. Section 3 contains the mathematical modelling that shows the use of the proposed MRAC technique as an MPPT controller of PV arrays. Section 4 shows the simulation results on a PV array model and compares the performance of the proposed controller with the performance of other two non-linear controllers used in the literature. The last section contains the concluding remarks and underlines some directions for future work.

2. The Proposed Model Reference Adaptive Control Approach

Based on the control systems theory concepts, the variables used in a mathematical model that represents an evolution during the time (denoted with t), are partitioned into:

- *state variables*, represented by the vector $\mathbf{x}(t)$, with cardinality $N_{\mathbf{x}}$;
- *control variables*, represented by the vector $\mathbf{u}(t)$, with cardinality $N_{\mathbf{u}}$;
- *algebraic variables*, represented by the vector $\mathbf{y}(t)$, with cardinality $N_{\mathbf{y}}$

The matrix-based model of the dynamic system is written with the following non-linear differential algebraic equations:

$$\dot{\mathbf{x}}(t) = \mathbf{f}(\mathbf{x}(t), \mathbf{u}(t)) \tag{1}$$

$$\mathbf{g}(\mathbf{x}(t)) = \mathbf{y}(t) \tag{2}$$

The concept of adaptive control considers the definition of a reference trajectory for the controlled variable, up to reaching the reference values for the output variable vector y_{r0} at the equilibrium point after the transient. The reference trajectory can be defined by considering user-based specifications on typical parameters of the dynamic response such as the rise time, the overshoot and the settling time [43].

At the equilibrium point, the state variable vector is indicated as $\mathbf{x}^*$ and the control variable vector as $\mathbf{u}^*$, so that (avoiding in the sequel the explicit indication of the dependence on time):

To guarantee that the adaptive control law results in an asymptotically stable equilibrium point, the following errors are considered:

- The errors with respect to the state variables:

$$\mathbf{e}_{\mathbf{x}} = \mathbf{A}(\mathbf{x} - \mathbf{x}^*) \tag{3}$$

- The errors with respect to the control variables:

$$\mathbf{e_u} = \mathbf{B}(\mathbf{u} - \mathbf{u}^*) \tag{4}$$

where **A** is the diagonal matrix that contains on the diagonal the weighting factors α_i referring to the errors on the state variables, for $i = 1,..., N_{\mathbf{x}}$, and **B** is the diagonal matrix that contains on the diagonal the weighting factors β_j referring to the errors on the control variables, for $j = 1,..., N_{\mathbf{u}}$. The entries in the diagonal matrices can be different to take into account the different units of the variables involved in the related equations, or the different variations that occur during the solution process.

The two types of errors are included in a single vector:

$$\mathbf{e} = [\mathbf{e}_{\mathbf{x}}^{\mathrm{T}}, \mathbf{e}_{\mathbf{u}}^{\mathrm{T}}]^{\mathrm{T}} \tag{5}$$

The key aspect for designing the model reference adaptive control is that the state vector **x** depends on the control variable vector **u**. The solution of the control problem requires the evaluation of the control variable vector $\mathbf{u}(t)$ to be provided as an input to the system for reducing to zero all the entries of the error vector, while satisfying the dynamic constraints. The controller design problem is then written as follows:

$$\dot{\mathbf{x}}(\mathbf{u}) = \mathbf{f}(\mathbf{x}(\mathbf{u}), \mathbf{u}) \tag{6}$$

$$\mathbf{e}(\mathbf{x}(\mathbf{u}), \mathbf{u}) = \mathbf{0} \tag{7}$$

The TCB approach is applied to guarantee the asymptotic stability of the equilibrium point [38]. For this purpose, the following scalar-positive semi-definite Lyapunov function is defined:

$$V = \frac{1}{2}\mathbf{e}^{\mathrm{T}}\mathbf{e} \tag{8}$$

and its derivative with respect to time is [8]:

$$\dot{V} = \mathbf{e}^{\mathrm{T}}\dot{\mathbf{e}} \tag{9}$$

Considering the following expression of $\dot{\mathbf{e}}$:

$$\dot{\mathbf{e}} = \frac{\partial \mathbf{e}}{\partial \mathbf{u}}\dot{\mathbf{u}} \tag{10}$$

the time derivative of V can also be written as:

$$\dot{V} = \mathbf{e}^{\mathrm{T}}\frac{\partial \mathbf{e}}{\partial \mathbf{u}}\dot{\mathbf{u}} \tag{11}$$

From the Lyapunov theorem, the asymptotic stability of the equilibrium point is guaranteed if $\dot{V}$ is negative-definite or negative semi-definite. In the TCB approach, the condition imposed is that the change of $\dot{\mathbf{u}}$ occurs in the direction of the gradient of V, considering a positive constant K:

$$\dot{\mathbf{u}} = -K \cdot \left(\frac{\partial V}{\partial \mathbf{u}}\right)^{\mathrm{T}} = -K \cdot \left(\frac{\partial \mathbf{e}}{\partial \mathbf{u}}\right)^{\mathrm{T}}\mathbf{e} \tag{12}$$

Then, the expression of the time derivative of V becomes:

$$\dot{V} = -K \cdot \mathbf{e}^{\mathrm{T}}\left(\frac{\partial \mathbf{e}}{\partial \mathbf{u}}\right)\left(\frac{\partial \mathbf{e}}{\partial \mathbf{u}}\right)^{\mathrm{T}}\mathbf{e} \tag{13}$$

and is structurally a negative semi-definite quadratic form. In this way, by generating the trajectory of the control variable vector $\mathbf{u}(t)$ according to Equation (12), the asymptotic stability of the equilibrium point is guaranteed.

3. Application of the MRAC-TCB Approach for MPPT of PV Arrays

3.1. PV System Overview

This section describes the MRAC-TCB control approach to realize a novel MPPT method in a PV system with a Buck-Boost converter as an interfacing switching topology between the PV source and the load. In the following, every part of the PV system considered is introduced and discussed.

The topology of the proposed stand-alone PV system is shown in Figure 2. The system consists of the following components:

- PV array
- Regression plane
- Non-inverted Buck-Boost converter
- MRAC-TCB controller

In the PV system, the sensors provide the values of the irradiance and temperature of the PV panel to the regression plane that determines the voltage at the MPP, termed as V_{MPP}, using a mathematical relationship. The error in the PV system is defined as the difference between the output voltage of the PV array and the reference voltage. This error is the input of the designed MRAC-TCB controller, which generates the output signal u that controls the duty ratio of the Buck-Boost converter through the use of a pulse width modulation (PWM) generator. Further details about the regression plane, the mathematical modelling of the converter, and the derivation of the controller, are given in the next subsections.

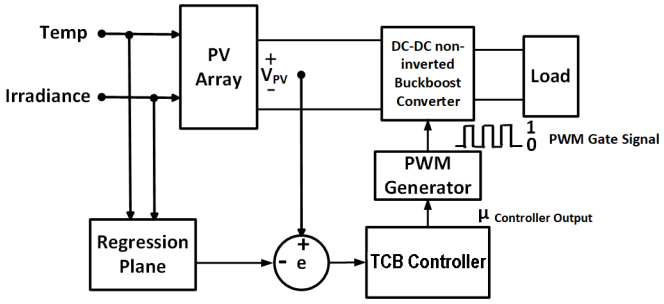

Figure 2. Block diagram of the PV system.

3.2. Generation of the Reference Voltage by the Regression Plane

The regression plane provides the value of V_{MPP} for any value of irradiance and temperature of the PV array. This is performed by establishing a linear mathematical relationship for the calculation of V_{MPP} from the values of irradiance and temperature. Examples of this methodology in the literature can be found in the Refs. [29,44]. In this paper, the relationship is established by the following process. First, multiple MPP curves are generated by varying the temperature from 30 °C to 60 °C at constant irradiance level of 1000 W/m^2, and their data points are recorded. Then, the temperature is kept constant at 25 °C and the level of irradiance is varied from 1000 W/m^2 to 600 W/m^2. In this way, another set of data points is generated. From the data points obtained, linear regression is applied to obtain a three-dimensional regression plane. From the regression plane, a value of V_{MPP} is obtained for any value of temperature and irradiance. Details of the PV array that have been used for the collection of data points are provided in Table 1. The mathematical relationship established between V_{MPP}, irradiance G and temperature T is as follows:

$$V_{MPP} = c_0 - c_T\, T - c_G\, G \tag{14}$$

where c_0, c_T and c_G are coefficients whose values are determined for each PV array individually.

Table 1. Specifications of PV array.

Description of Parameters	Nominal Value
PV modules per string	10
Parallel strings	1
Maximum Power	213.15 W
Cells per module	72
Voltage at open circuit	363 V
Current at short circuit	7.84 A
Voltage at Maximum Power	290 V
Current at Maximum Power	7.35 A

3.3. Mathematical Modeling of the Non-Inverted Buck-Boost Converter

The inclusion of a DC–DC converter is necessary in a PV system, because it provides the interface between the PV panel and the load and enables the tracking of the operating point of the PV panel to its MPP. In this paper, a Non-inverted Buck-Boost converter is used, because from all the proposed converters it is considered one of the best choices for MPPT applications [45]. Comparing different types of converters is outside the scope of this paper, and the proposed technique is applicable to all the types of converters. The circuit diagram of the converter is shown in Figure 3. In this paper, the converter is operated with continuous conduction only.

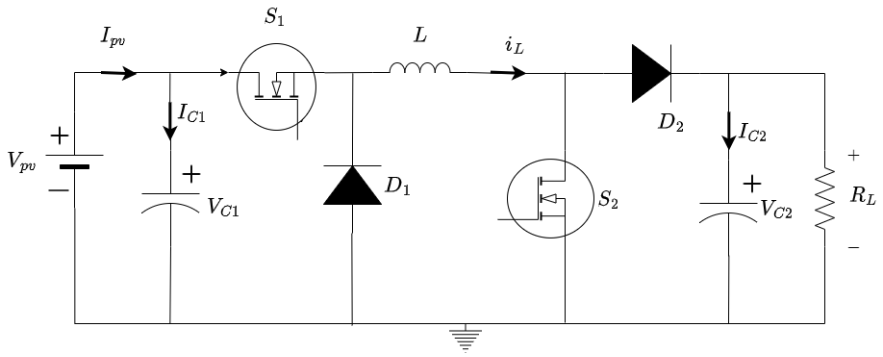

Figure 3. Non-inverted Buck-Boost converter.

The converter has two modes of operation. In the first mode, the switches are ON, and the diode is reverse-biased. Using Kirchhoff's current and voltage laws, the equations for the capacitor current and inductor voltage in the first mode of operation are:

$$\begin{cases} i_{C1} = i_{PV} - i_L \\ v_L = v_{C1} \\ i_{C2} = -\dfrac{v_{C2}}{R} \end{cases} \tag{15}$$

In the second mode, both switches are OFF and the diode is forward-biased. Again, using Kirchhoff's voltage and current laws, the equations for the capacitor current and inductor voltage are:

$$\begin{cases} i_{C1} = i_{PV} \\ v_L = -v_{C2} \\ i_{C2} = i_{L1} - \dfrac{v_{C2}}{R} \end{cases} \tag{16}$$

Using the volt-second balance on the inductor L and the capacitor charge balance on the capacitors C_1 and C_2, and denoting as μ the average value of the duty ratio, the following equations are derived:

$$\begin{cases} \frac{dv_{C1}}{dt} = \frac{i_{PV}}{C_1} - \frac{i_L}{C_1}\mu \\ \frac{di_L}{dt} = \frac{v_{C1}}{L}\mu - \frac{v_{C2}}{L}(1-\mu) \\ \frac{dv_{C2}}{dt} = \frac{i_L}{C_2}(1-\mu) - \frac{v_{C2}}{R_{C2}} \end{cases} \tag{17}$$

Let x_1, x_2 and x_3 be the average values of v_{C1}, i_L and v_{C2}, respectively:

$$\begin{cases} x_1 = v_{C1} \\ x_2 = i_L \\ x_3 = v_{C2} \end{cases} \tag{18}$$

The average duty cycle μ is taken as the control variable u, which is the single entry of the control variable vector $\mathbf{u}$ defined in Section 2. By replacing in Equation (17) the state variables defined in (18) and the control variable u, the following equations can be derived:

$$\begin{cases} \dot{x}_1 = \frac{i_{PV}}{C_1} - \frac{x_2}{C_1}u \\ \dot{x}_2 = \frac{x_1}{L}u - \frac{x_3}{L}(1-u) \\ \dot{x}_3 = \frac{x_2}{C_2}(1-u) - \frac{x_3}{RC_2} \end{cases} \tag{19}$$

The above state space model is used to track the reference V_{MPP}.

3.4. Mathematical Derivation of the MRAC-TCB Approach for the Non-Inverted Buck-Boost Converter

Again, the procedure to apply the MRAC-TCB controller follows the same methodology as the previous sections. The first step is the derivation of a reference signal for the trajectory to follow. As explained above, this is generated through the use of a regression plane. Again, this means that for this particular application the variable of interest y_{r0} is defined as v_{C1}.

The second step is the derivation of the steady-state expressions for all the states of the system. These expressions are found by setting the contents of Equation (19) to zero.

$$\begin{cases} x_1^* = y_{r0} \\ u^* = \frac{2a - \sqrt{4a^2 - 4a(a-y_{r0})}}{2(a-y_{r0})} \\ x_2^* = \frac{y_{r0}u^*}{R(1-u^*)^2} \\ x_3^* = \frac{y_{r0}u^*}{1-u^*} \end{cases} \tag{20}$$

where $a = I_{pv}R_1$.

The next step is to define the tracking errors that can be minimized through the adaptation mechanism to accurately track the reference signal, as:

$$\begin{cases} e_{x_1} = \alpha_1(x_1 - x_1^*) \\ e_{x_2} = \alpha_2(x_2 - x_2^*) \\ e_{x_3} = \alpha_3(x_3 - x_3^*) \\ e_u = \beta(u - u^*) \end{cases} \tag{21}$$

Here, the weight vector entries α_1, α_2 and α_3 of the diagonal matrix **A** and the weight constant β are empirically determined to specify the speed of the control algorithm. Again, using the expression defined in Equation (12) and the error vector mentioned above, the control equation becomes:

$$\dot{u} = -K\left[\alpha_1 \frac{dx_1}{du} e_{x_1} + \alpha_2 \frac{dx_2}{du} e_{x_2} + \alpha_3 \frac{dx_3}{du} e_{x_3} + \beta e_u\right] \tag{22}$$

where K is the gain factor with a constant value given in Table 2. The sensitivity parameters $s_1 = \frac{dx_1}{du}$, $s_2 = \frac{dx_2}{du}$ and $s_3 = \frac{dx_3}{du}$ are calculated based on the original Buck-Boost converter model given in Equation (17).

$$\begin{cases} \dot{s}_1 = -\frac{1}{C_1}(-x_2 - s_2 u) \\ \dot{s}_2 = -\frac{1}{L}(s_1 u + x_3 - s_3(1-u) + x_1) \\ \dot{s}_3 = \frac{1}{C_2}\left(s_2(1-u) - x_2 - \frac{s_3}{R}\right) \end{cases} \tag{23}$$

Table 2. Specifications of Buck-Boost converter and controller gains.

Description of Parameters	Nominal Value
Capacitance, C_1	67 µF
Capacitance, C_2	480 µF
Inductance, L	11 mH
Resistance, R	20 Ω
Switching frequency, f_s	100 kHz
TCB gain, K	10^4

3.5. Simulation Results for the Buck-Boost Converter

The proposed MRAC-TCB controller has been tested by imposing both fluctuating and step-wise changes in the environmental conditions of irradiance, with simulations carried out in Matlab/Simulink. The irradiance can be gathered at fast rates, for example, second by second or even at sub-second rates [46]. Therefore, the testing is carried out by applying step irradiance changes pushed to very large changes as a conservative stress case. In particular, while the irradiance values are kept within a reasonable range, the controller has been intentionally subject to large changes at very fast time steps, to impose higher stress to the control system with respect to actual conditions in which the corresponding quantities could change more smoothly. The results are presented in the next subsection. Concerning temperature changes, these changes occur at a slower rate [47], so that no testing is shown for temperature variations in the sub-second observation time interval considered.

In the specifications for the PV array and Buck-Boost converter mentioned in Tables 1 and 2, respectively, the empirically determined values of weight vector is **A** is [3,1,1] and the weight β is equal to 5. To justify the selection of these parameters, we have shown the evolution of the steady-state errors with respect to the values of the weight vector entries and of the controller gain K in Figure 4. As seen from Figure 4a,c, as the value of α_1 and β is increased, the steady-state errors of all parameters are reduced. Similarly, Figure 4b,c shows that as the value of K is increased to 1×10^4, errors are also reduced more smoothly. Therefore, the choice of all weight vector entries equal to unity is not the best one, and the increase in the value of K is justified as well. Further increasing the value of K does not provide significant additional benefits.

Considering the values α_1, α_2, α_3, and β, being four entries involved, a unique representation of the combinations of values of these entries is not possible. Hence, the description of the parameters chosen has been conducted as follows. The error on the control variable related to β is considerably lower with respect to the errors in the other variables. In particular, from Figure 4, when $\beta = 1$ there are some fluctuations in the error (as shown in Figure 4), and these fluctuations are progressively reduced when β increases (and this

happens with different combinations of α_1, α_2 and α_3). For values of β around 5 or higher the fluctuations remain very small, so that the value chosen is $\beta = 5$ and is maintained for the other tests shown.

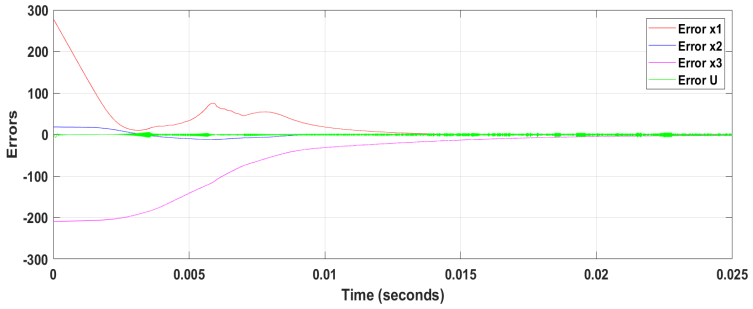

(**a**)

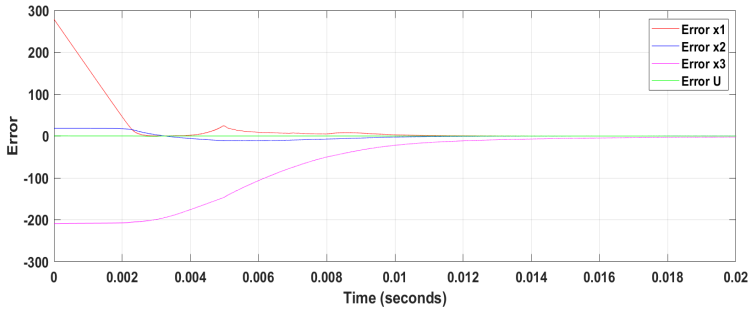

(**b**)

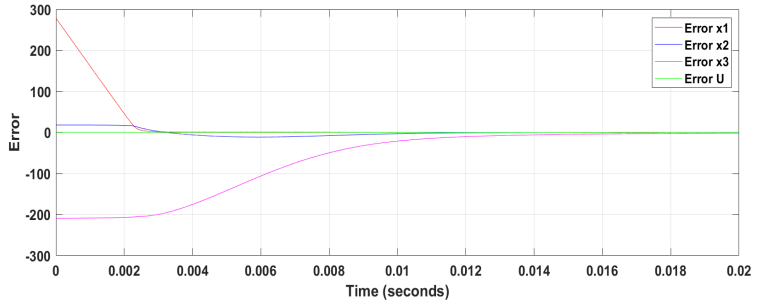

(**c**)

Figure 4. Evolution of errors w.r.t. variations in the parameters. (**a**) All weight vector entries equal to *unity*, and parameter $K = 1 \times 10^4$. (**b**) Weight vector entries $\alpha_1 = 3$, $\alpha_2 = 1$, $\alpha_3 = 1$, $\beta = 5$, and parameter $K = 1 \times 10^3$. (**c**) Weight vector entries $\alpha_1 = 3$, $\alpha_2 = 1$, $\alpha_3 = 1$, $\beta = 5$, and parameter $K = 1 \times 10^4$.

About the values of α_1, α_2 and α_3, the comparison has been carried out by keeping $\alpha_3 = 1$ and changing the values of α_1 and α_2. A parametric analysis with α_1 and α_2 variable from 0.5 to 5 is shown in the 3D graph of Figure 5a, referring to the 2% settling time as the entry used for comparison. Looking at the trend of variation of the 2% settling time, the values $\alpha_1 = 3$ and $\alpha_2 = 1$ (indicated with the red ellipses and arrow) are chosen based on the application of the elbow criterion, for which the changes in the 2% settling time become acceptably low.

Figure 5b–e shows how changing the values of α_1 and α_2 does not result in a significant change in the errors of the parameters x_1 and x_2 after the first part of the evolution. Each error has been normalized by dividing the parameter values with the total change in error from the starting point to the steady-state conditions.

The numerical values of the coefficients of the regression plane for this PV array system, determined as indicated in Section 3.2, are $c_0 = 322$, $c_T = 1.34$, and $c_G = 0.00964$.

The final subsection presents the comparison of the MRAC-TCB controller with an integral back-stepping and a P&O controller.

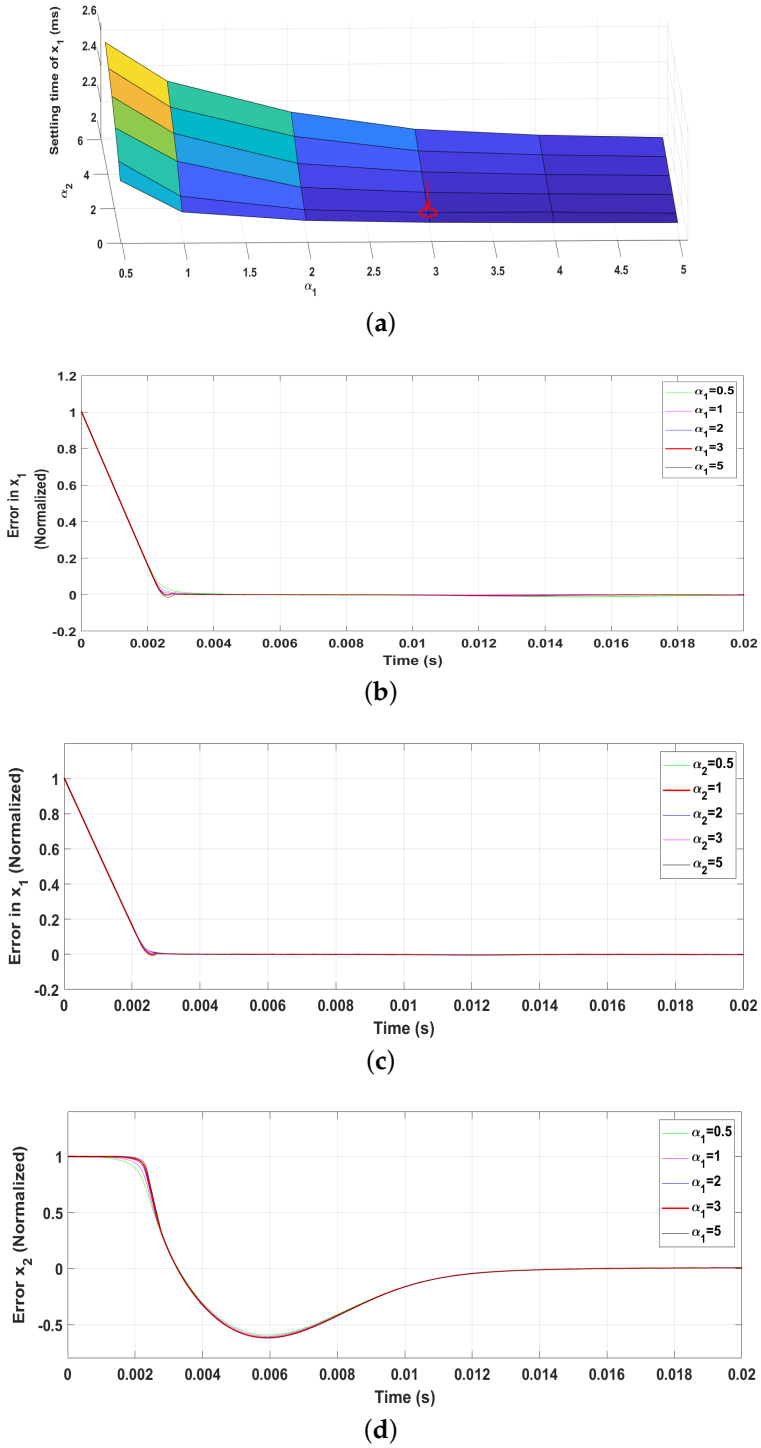

Figure 5. *Cont.*

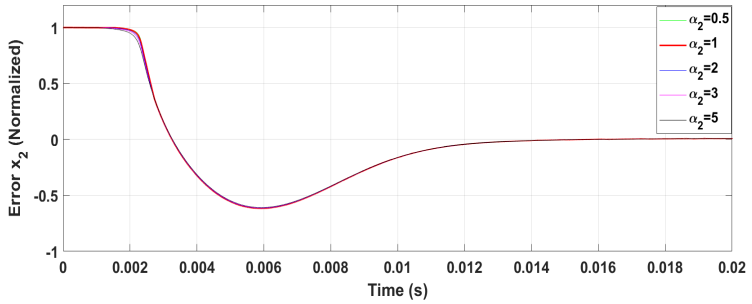

(**e**)

Figure 5. Evolution of errors in x_1 and x_2 parameters w.r.t. variations in α_1 and α_2 and settling time in x_1. (**a**) Variation in settling time (2%) of x_1 due to variations in α_1 and α_2. (**b**) Error in x_1 due to variations in α_1 while α_2 is 1. (**c**) Error in x_1 due to variations in α_2 while α_1 is 3. (**d**) Error in x_2 due to variations in α_1 while α_2 is 1. (**e**) Error in x_2 due to variations in α_2 while α_1 is 3.

Test under Conditions of Variable Irradiance

The controller was tested under conditions of variable irradiance. Initially, the irradiance values changed in a fluctuating way, while the temperature was kept constant at 25 °C. This is shown in Figure 6. The fluctuations centered around 1000 W/m^2 and ranged from 900 to 1140 W/m^2. In the second test, shown in Figure 7 the range of irradiance change increased by a large margin to test the stability and the sensitivity of our controller gains to large variations. Furthermore, the irradiance change was performed in a step-wise manner to subject our controller to the strongest form of stress. The initial irradiance is kept at 1000 W/m^2, and is changed in a step-wise way to 800 W/m^2 at 0.05 s. This value is then further stepped down to 600 W/m^2 at 0.15 s.

Figures 8 and 9 show the reference voltage tracking under both fluctuating and step-wise variable irradiance conditions. The first aspect to note is that the generated reference value from the regression plane is tracked efficiently, due to the controller with no steady-state error. The controller is not only able to track the sudden change in reference voltage due to fluctuations in Figure 8, but is also able to track the large and sudden step-wise changes in irradiance at 0.05 s and 1 s, respectively with minute rise and settling times. Figure 10 shows both the maximum power-point tracking and the output power generated by the proposed MRAC-TCB controller under the step change variable irradiance conditions. From Figure 10, the generated power output of the PV array is delivered to the load with MPPT efficiency above 95%.

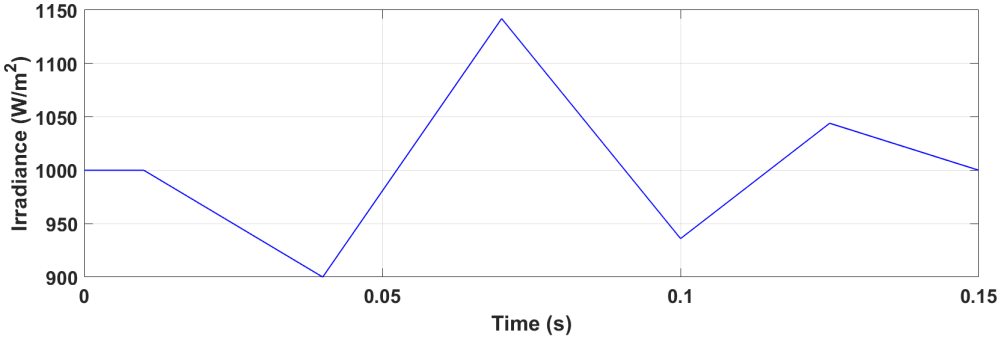

Figure 6. Test with fluctuating irradiance in time.

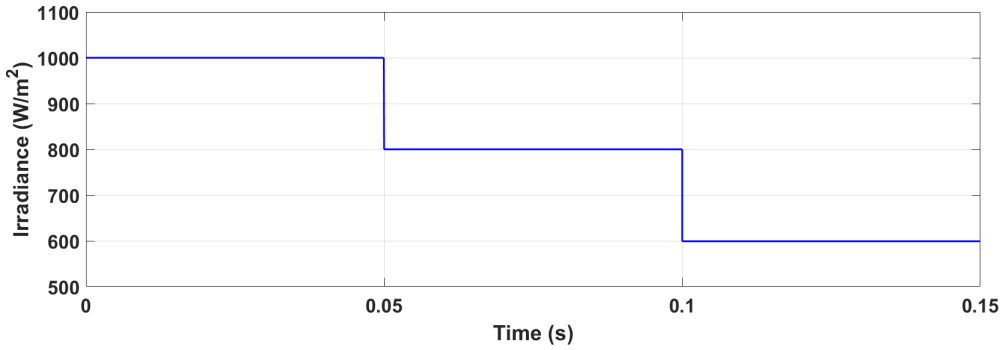

Figure 7. Test with step-wise variable irradiance in time.

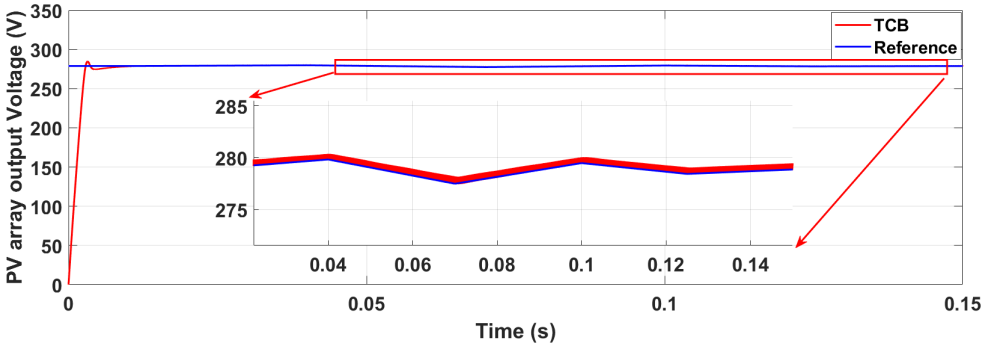

Figure 8. Tracking the MPP voltage under fluctuating irradiance.

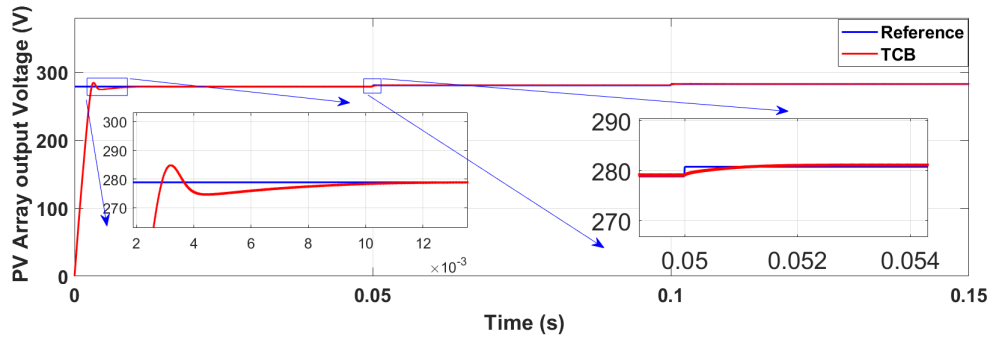

Figure 9. Tracking the MPP voltage under step-wise variable irradiance.

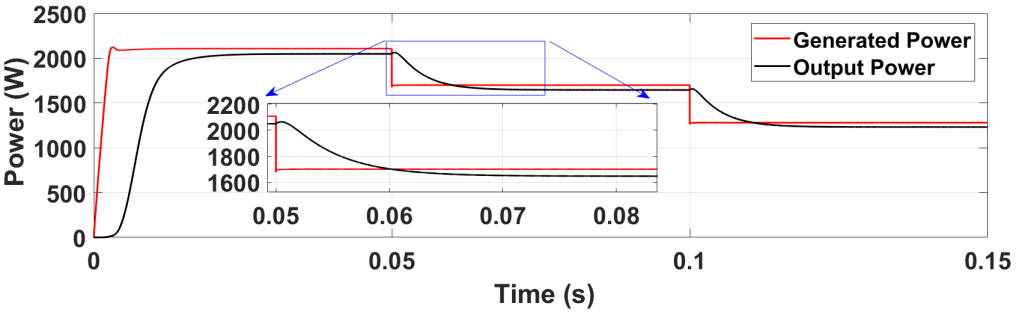

Figure 10. Power output of the PV Array under step-wise variable irradiance.

3.6. Comparison with Perturb and Observe and Integral Back-Stepping Controllers

Among the non-linear controllers implemented in the literature, one of the best results was cited by the Ref. [30] for an MPPT system based on a non-inverted Buck-Boost system. Therefore, for comparison purposes, the *integral back-stepping* (IBS) controller proposed in the Ref. [30] has been replicated and a comparison with the proposed controller has been carried out. In addition, a simple P&O controller has been fine-tuned as well for the

PV system under analysis. Figure 11 shows the tracking of the reference voltage of the three controllers under conditions of step-wise varying irradiance. It can be seen from the figure that the MRAC-TCB and the IBS controllers have no issues of steady-state errors, although the IBS controller has slight voltage overshoot.

A comparison between the responses of these controllers is provided in Table 3. While the IBS controller has a slight overshoot of around 13 V and a settling time (2%) of 2.7 ms, the MRAC-TCB controller can be fine-tuned to have almost no overshoot voltage and a settling time (2%) of 3.1 ms. Even after perturbations, as can be seen in Figure 11, the response of TCB controller settles down much quicker than that of the IBS controller. Furthermore, after the perturbations, the MRAC-TCB controller also has a rise time of only 54.75 µs, as compared to 2.17 ms of the IBS controller.

Similarly, Figure 12 shows that after multiple fine tuning attempts, P&O can also track the MPPT point but undergoes several fluctuations before reaching the steady-state point. While it should be noted the P&O is the simplest controller to implement as it does not require the use of a regression plane and hence the extra sensors, the superiority of Lyapunov-based controllers is evident. In particular, the settling time (2%) of P&O cannot be determined because the output voltage value does not reach 2% of the steady-state value.

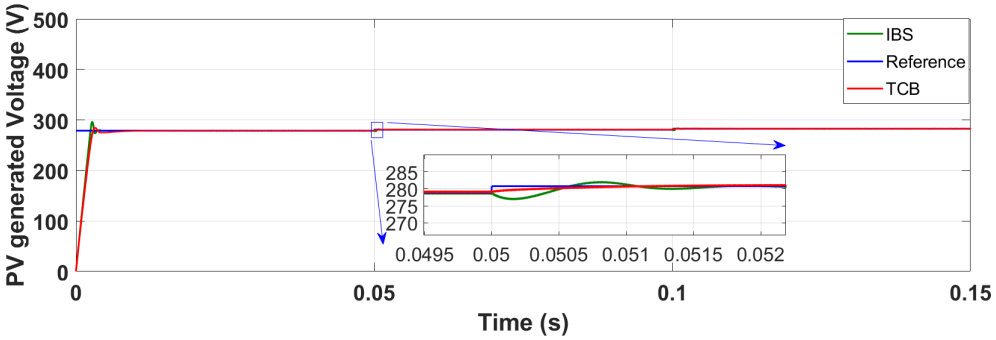

Figure 11. PV array MPP voltage tracking comparison with the IBS controller under variable irradiance.

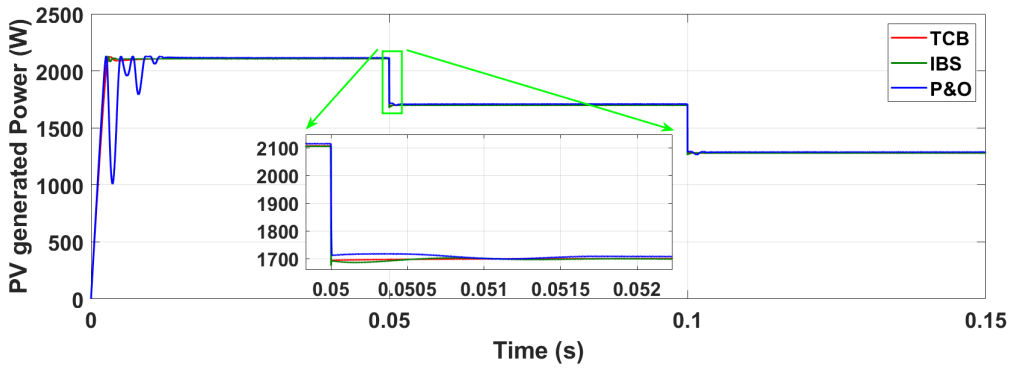

Figure 12. PV array MPPT comparison with the IBS and P&O controllers under variable irradiance.

Table 3. Comparison between controllers.

Method	RT (ms)	ST 5% (ms)	ST 2% (ms)	Overshoot (V)	MPPT Efficiency
P&O	2.3	58.2	NA	86.0	94.8
IBS	2.1	2.8	2.7	13.3	97.4
MRAC-TCB	2.3	2.5	3.0	6.3	96.8

4. Conclusions

In this paper, a pulse-width-modulated, model reference adaptive control based on the TCB controller was proposed for the regulation of an inverted Buck-Boost converter applied as a maximum power-point tracker in a PV system. This paper has demonstrated for the first time the application of the MRAC-TCB controller to the inverted Buck-Boost converter taken as a viable example of a converter for the specific application. Nevertheless, the proposed control technique is applicable to all types of DC–DC converters. The proposed controller has demonstrated strong robustness under various testing conditions, confirming the theoretical findings that prove the global asymptotic stability using the Lyapunov stability criterion.

The simulations of the PV system were performed in a Matlab/Simulink environment. The regression plane was used to generate the peak power voltage taken as reference for the MRAC-TCB controller. The tests were carried out by using variable irradiance with large and step-wise changes at fast rates, that is, the changes imposed were larger with respect to what would happen in real conditions that could be tested experimentally. Even by imposing these stress cases in the simulations, the MRAC-TCB controller exhibited a very robust response. Moreover, the test with fluctuating irradiance in time has shown effective adaptation of the output voltage to the changing external conditions.

From the results of further comparisons with the Lyapunov-based Integral Back-Stepping controller and a P&O controller, referring to settling time, voltage overshoot and MPPT efficiency, the MRAC-TCB controller exhibited results clearly better than P&O and comparable with the Integral Back-Stepping controller, in particular, with remarkably lower voltage overshoot.

It should be noted that, although the controller performance is excellent, the results are dependent on the accuracy and precision in the definition of the regression plane. For practical applications, as the PV array ages, the regression plane may need to be updated.

Work is in progress to extend the study to the comparison of the results obtained with the proposed MRAC-TC controller to different converters and to test the proposed controller in real-case applications.

Author Contributions: Conceptualization, M.A.Q., F.T. and G.C.; methodology, M.A.Q., F.T., S.M. and A.R.; software, M.A.Q.; validation, S.M., A.R., A.M. and G.C.; formal analysis, M.A.Q., F.T., S.M., A.R., A.M. and G.C.; writing—original draft preparation, M.A.Q. and G.C.; writing—review and editing, M.A.Q., F.T., S.M., A.R., A.M. and G.C. All authors have read and agreed to the published version of the manuscript.

Funding: S.M. and A.R. acknowledge the Nationally funded research project (PRIN) entitled Innovative Solutions for Renewables in Energy Communities (ISoREC).

Data Availability Statement: The data presented in this study are available on request from the first author.

Conflicts of Interest: The authors declare no conflict of interest.

Abbreviations

AI	Artificial intelligence
DC	Direct current
FL	Fuzzy logic
GMPP	Global maximum power-point
IBS	Integral back-stepping controller
IC	Incremental conductance
ISMC	Integral sliding mode control
LMPP	Local maximum power-point
MPP	Maximum power-point

MPPT	Maximum power-point tracking
MRAC	Model reference adaptive control
NN	Neural network
PID	Proportional integral derivative
P&O	Perturb and observe
PV	Photovoltaic
PWM	Pulse width modulation
SMC	Sliding mode control
TCB	Torelli control box

References

1. Padmanathan, K.; Govindarajan, U.; Ramachandaramurthy, V.K.; Jeevarathinam, B. Integrating solar photovoltaic energy conversion systems into industrial and commercial electrical energy utilization—A survey. *J. Ind. Inf. Integr.* **2018**, *10*, 39–54.
2. Cavallaro, C.; Musumeci, S.; Santonocito, C.; Pappalardo, M. Smart photovoltaic UPS system for domestic appliances. In Proceedings of the IEEE 2009 International Conference on Clean Electrical Power, Capri, Italy, 9–11 June 2009; pp. 699–704.
3. Fahmi, M.; Rajkumar, R.; Arelhi, R.; Isa, D. Solar PV system for off-grid electrification in rural area. In Proceedings of the 3rd IET International Conference on Clean Energy and Technology (CEAT) 2014, Kuching, Malaysia, 24–26 November 2014.
4. Awasthi, A.; Sinha, A.; Singh, A.K.; Veeraganesan, R. Solar PV fed grid integration with energy storage system for electric traction application. In Proceedings of the IEEE 2016 10th International Conference on Intelligent Systems and Control (ISCO), Coimbatore, India, 7–8 January 2016; pp. 1–5.
5. Liu, N.; Cheng, M. Effectiveness evaluation for a commercialized pv-assisted charging station. *Sustainability* **2017**, *9*, 323. [CrossRef]
6. Nadeem, F.; Hussain, S.S.; Tiwari, P.K.; Goswami, A.K.; Ustun, T.S. Comparative review of energy storage systems, their roles, and impacts on future power systems. *IEEE Access* **2018**, *7*, 4555–4585. [CrossRef]
7. Beriber, D.; Talha, A. MPPT techniques for PV systems. In Proceedings of the IEEE 4th International Conference on Power Engineering, Energy and Electrical Drives, Istanbul, Turkey, 13–17 May 2013; pp. 1437–1442.
8. Bakhiyi, B.; Labrèche, F.; Zayed, J. The photovoltaic industry on the path to a sustainable future—Environmental and occupational health issues. *Environ. Int.* **2014**, *73*, 224–234. [CrossRef]
9. Chimento, F.; Musumeci, S.; Raciti, A.; Sapuppo, C.; Di Guardo, M. A control algorithm for power converters in the field of photovoltaic applications. In Proceedings of the IEEE 2007 European Conference on Power Electronics and Applications, Aalborg, Denmark, 2–5 September 2007; pp. 1–9.
10. Sarvi, M.; Azadian, A. A comprehensive review and classified comparison of MPPT algorithms in PV systems. *Energy Syst.* **2022**, *13*, 281–320. [CrossRef]
11. Derbeli, M.; Napole, C.; Barambones, O.; Sanchez, J.; Calvo, I.; Fernández-Bustamante, P. Maximum power-point Tracking Techniques for Photovoltaic Panel: A Review and Experimental Applications. *Energies* **2021**, *14*, 7806. [CrossRef]
12. Gil-Antonio, L.; Saldivar-Marquez, M.B.; Portillo-Rodriguez, O. Maximum power-point tracking techniques in photovoltaic systems: A brief review. In Proceedings of the IEEE 2016 13th International Conference on Power Electronics (CIEP), Guanajuato, Mexico, 20–23 June 2016; pp. 317–322.
13. Koutroulis, E.; Blaabjerg, F. A new technique for tracking the global maximum power-point of PV arrays operating under partial-shading conditions. *IEEE J. Photovolt.* **2012**, *2*, 184–190. [CrossRef]
14. Nguyen, T.L.; Low, K.S. A global maximum power-point tracking scheme employing DIRECT search algorithm for photovoltaic systems. *IEEE Trans. Ind. Electron.* **2010**, *57*, 3456–3467. [CrossRef]
15. Lian, K.; Jhang, J.; Tian, I. A maximum power-point tracking method based on perturb-and-observe combined with particle swarm optimization. *IEEE J. Photovolt.* **2014**, *4*, 626–633. [CrossRef]
16. Sundareswaran, K.; Vigneshkumar, V.; Sankar, P.; Simon, S.P.; Nayak, P.S.R.; Palani, S. Development of an improved P&O algorithm assisted through a colony of foraging ants for MPPT in PV system. *IEEE Trans. Ind. Inform.* **2015**, *12*, 187–200.
17. Gupta, A.K.; Pachauri, R.K.; Maity, T.; Chauhan, Y.K.; Mahela, O.P.; Khan, B.; Gupta, P.K. Effect of various incremental conductance MPPT methods on the charging of battery load feed by solar panel. *IEEE Access* **2021**, *9*, 90977–90988. [CrossRef]
18. Ji, Y.H.; Jung, D.Y.; Kim, J.G.; Kim, J.H.; Lee, T.W.; Won, C.Y. A real maximum power-point tracking method for mismatching compensation in PV array under partially shaded conditions. *IEEE Trans. Power Electron.* **2010**, *26*, 1001–1009. [CrossRef]
19. Mateo Romero, H.F.; González Rebollo, M.Á.; Cardeñoso-Payo, V.; Alonso Gómez, V.; Redondo Plaza, A.; Moyo, R.T.; Hernández-Callejo, L. Applications of artificial intelligence to photovoltaic systems: A review. *Appl. Sci.* **2022**, *12*, 10056. [CrossRef]
20. Kermadi, M.; Salam, Z.; Eltamaly, A.M.; Ahmed, J.; Mekhilef, S.; Larbes, C.; Berkouk, E.M. Recent developments of MPPT techniques for PV systems under partial shading conditions: A critical review and performance evaluation. *IET Renew. Power Gener.* **2020**, *14*, 3401–3417. [CrossRef]
21. Podder, A.K.; Roy, N.K.; Pota, H.R. MPPT methods for solar PV systems: A critical review based on tracking nature. *IET Renew. Power Gener.* **2019**, *13*, 1615–1632. [CrossRef]
22. Khan, Z.A.; Khan, L.; Ahmad, S.; Mumtaz, S.; Jafar, M.; Khan, Q. RBF neural network based backstepping terminal sliding mode MPPT control technique for PV system. *PLoS ONE* **2021**, *16*, e0249705. [CrossRef] [PubMed]

23. Eltamaly, A.M. A novel musical chairs algorithm applied for MPPT of PV systems. *Renew. Sustain. Energy Rev.* **2021**, *146*, 111135. [CrossRef]
24. Mingyu, L.; Xinhong, C.; Bingyu, C. Random inertia weight PSO based MPPT for Solar PV under Partial Shaded Condition. In *Proceedings of the IOP Conference Series: Earth and Environmental Science*; IOP Publishing: Bristol, UK, 2020; Volume 585, p. 012028.
25. Abdellatif, W.S.; Mohamed, M.S.; Barakat, S.; Brisha, A. A Fuzzy Logic Controller Based MPPT Technique for Photovoltaic Generation System. *Int. J. Electr. Eng. Inform.* **2021**, *13*, 394–417.
26. Shinde, A.B.; Deshpande, A.S.; Unde, S. Design and Simulation of Self-tuning PID controller with MPPT for Solar Array using MATLAB/Simulink. In Proceedings of the 2022 13th International Conference on Computing Communication and Networking Technologies (ICCCNT), Kharagpur, India, 3–5 October 2022; pp. 1–6. [CrossRef]
27. Ghosh, A.; Malla, S.G.; Bhende, C.N. Small-signal modelling and control of photovoltaic based water pumping system. *ISA Trans.* **2015**, *57*, 382–389. [CrossRef] [PubMed]
28. Qureshi, M.A.; Ahmad, I.; Munir, M.F. Double integral sliding mode control of continuous gain four quadrant quasi-Z-source converter. *IEEE Access* **2018**, *6*, 77785–77795. [CrossRef]
29. Armghan, H.; Ahmad, I.; Armghan, A.; Khan, S.; Arsalan, M. Backstepping based non-linear control for maximum power-point tracking in photovoltaic system. *Solar Energy* **2018**, *159*, 134–141.
30. Arsalan, M.; Iftikhar, R.; Ahmad, I.; Hasan, A.; Sabahat, K.; Javeria, A. MPPT for photovoltaic system using nonlinear backstepping controller with integral action. *Solar Energy* **2018**, *170*, 192–200. [CrossRef]
31. Alsumiri, M.; Jiang, L. Sliding Mode Maximum power-point Tracking Controller for Photovoltaic Energy Conversion System with a SEPIC Converter. In *Proceedings of the Eighth Saudi Students Conference in the UK*; World Scientific: Singapore, 2016; pp. 463–475.
32. Tan, S.C.; Lai, Y.M.; Chi, K.T.; Martínez-Salamero, L.; Wu, C.K. A fast-response sliding-mode controller for boost-type converters with a wide range of operating conditions. *IEEE Trans. Ind. Electron.* **2007**, *54*, 3276–3286. [CrossRef]
33. Tan, S.C.; Lai, Y. Constant-frequency reduced-state sliding mode current controller for Cuk converters. *IET Power Electron.* **2008**, *1*, 466–477. [CrossRef]
34. Yang, T.; Sun, N.; Fang, Y.; Xin, X.; Chen, H. New adaptive control methods for n-Link robot manipulators with online gravity compensation: Design and experiments. *IEEE Trans. Ind. Electron.* **2021**, *69*, 539–548. [CrossRef]
35. Sun, L. Helicopter Hovering Control Design based on Model Reference Adaptive Method. In Proceedings of the 2019 IEEE 3rd Information Technology, Networking, Electronic and Automation Control Conference (ITNEC), Chengdu, China, 15–17 March 2019; pp. 1621–1624.
36. Morse, W.; Ossman, K. Model following reconfigurable flight control system for the AFTI/F-16. *J. Guid. Control Dyn.* **1990**, *13*, 969–976. [CrossRef]
37. Safamehr, H.; Najafabadi, T.A.; Salmasi, F.R. Adaptive Control of Grid-Connected Inverters With Nonlinear LC Filters. *IEEE Trans. Power Electron.* **2023**, *38*, 1562–1570. [CrossRef]
38. Torelli, F.; Vaccaro, A. A generalized computing paradigm based on artificial dynamic models for mathematical programming. *Soft Comput.* **2014**, *18*, 1561–1573. [CrossRef]
39. Xie, N.; Torelli, F.; Bompard, E.; Vaccaro, A. Dynamic computing paradigm for comprehensive power flow analysis. *IET Gener. Transm. Distrib.* **2013**, *7*, 832–842. [CrossRef]
40. Torelli, F.; Vaccaro, A.; Xie, N. A novel optimal power flow formulation based on the Lyapunov theory. *IEEE Trans. Power Syst.* **2013**, *28*, 4405–4415. [CrossRef]
41. Torelli, F.; Montegiglio, P.; De Bonis, A.; Catalão, J.P.; Chicco, G.; Mazza, A. A new approach for solving DAE systems applied to distribution networks. In Proceedings of the IEEE 2014 49th International Universities Power Engineering Conference (UPEC), Cluj-Napoca, Romania, 22–25 September 2014; pp. 1–6.
42. Qureshi, M.A.; Torelli, F.; Mazza, A.; Chicco, G. Application of artificial dynamics to represent non-isolated single-input multiple-output DC–DC converters with averaged models. In Proceedings of the IEEE 2021 56th International Universities Power Engineering Conference (UPEC), Virtual, 31 August–3 September 2021; pp. 1–6.
43. Djaferis, T.E.; Schick, I.C. *System Theory: Modeling, Analysis and Control*; Springer: New York, NY, USA, 2012.
44. Iftikhar, R.; Ahmad, I.; Arsalan, M.; Naz, N.; Ali, N.; Armghan, H. MPPT for photovoltaic system using nonlinear controller. *Int. J. Photoenergy* **2018**, *2018*, 6979723. [CrossRef]
45. Başoğlu, M.E.; Çakır, B. Comparisons of MPPT performances of isolated and non-isolated DC–DC converters by using a new approach. *Renew. Sustain. Energy Rev.* **2016**, *60*, 1100–1113. [CrossRef]
46. Zurbriggen, I.G.; Ordonez, M. PV Energy Harvesting Under Extremely Fast Changing Irradiance: State-Plane Direct MPPT. *IEEE Trans. Ind. Electron.* **2019**, *66*, 1852–1861. [CrossRef]
47. Marinkov, S.; de Jager, B.; Steinbuch, M. Extremum seeking control with data-based disturbance feedforward. In Proceedings of the 2014 American Control Conference, Portland, OR, USA, 4–6 June 2014; pp. 3627–3632. [CrossRef]